KSCE Journal of Civil Engineering
Vol. 7, No. 1 / January 2003
pp. 33~39

Two-Dimensional Seismic Response Analysis of Basin Effects

By Min-Kyu Kim* Jong-Seh Lee, and Moon-Kyum Kim*****

Abstract

The site effect of local geological conditions on seismic ground motion is of great importance in earthquake engineering. An analytical method is presented herein to study the basin effect for layered soil systems. The method is based on a coupling of the finite element method and the boundary element method. The near field is modeled by the finite elements whereas the far field is modeled by the boundary element formulation using the multi-layer dynamic fundamental solution that satisfies the radiation condition of waves. In order to validate the analytical approach, a one-dimensional problem is modeled and the results are compared with those of a well-known SHAKE code. Two dimensional seismic response analyses are then performed for various ground systems to study the basin effect. Effects of the ground geometry and material contrast on the seismic responses are discussed in some details.

Keywords : *basin effect, dynamic fundamental solution, FE-BE coupling method, layered media, seismic response analysis*

1. Introduction

One of the most important and commonly encountered problems in earthquake engineering is the evaluation of ground responses due to seismic loading. Ground response analyses are used to predict ground surface motions for development of design response spectra, to evaluate dynamic stresses and strains for evaluation of liquefaction hazards, and to determine the earthquake induced forces that can lead to instability of earth and earth retaining structures.

Under ideal conditions, a complete ground response analysis would model the rupture mechanism at the source of an earthquake and the propagation of stress waves through the earth to the top of bedrock beneath a particular site, and then determine how the ground surface motion is influenced by the soil that lies above the bedrock. In reality, however, the mechanism of fault rupture is so complicated and the nature of energy transmission between the source and the site so uncertain that this approach is not practical for common engineering applications. The problem of ground response analyses then becomes one of determining the response of the soil deposit to the motion of the bedrock immediately beneath it. Despite the fact that seismic waves may travel through tens of kilometers of rock and often less than 100m of soil, the soil plays a very important role in determining the characteristics of the ground surface motion. It has long been recognized that local geological conditions can strongly influence the ground motion during earthquakes (Bielak and Ghattas, 1999). The importance of the effect became apparent during the 1985 Michoacan earthquake which caused widespread damages in Mexico City at a distance of 400 km from the epicenter. Damages were extensive to structures located within the lakebed region, but were minimal or nonexistent outside the soft soil deposits (Reinoso, 1997).

Since the 1920s, seismologists and, more recently, geotechnical earthquake engineers have worked toward the development of quantitative methods for predicting the influence of local soil conditions on strong ground motions. Over the years, a number of techniques have been developed and used for ground response analysis (Bielak *et al*., 1999) and have met with varying decrees of success. The techniques are often grouped depending on the dimensionality of the problems that they can address as documented in Bielak *et al*. (2000).

Recently, Kim *et al*. (2000) presented a dynamic fundamental solution for multi-layered half plane. Based on the

*Member, Hanyang University, Post doctorial Researcher (E-mail: minkyu76@msn.com)
**Member, Hanyang University, Professor (E-mail: jonglee@hanyang.ac.kr)
***Member, Yonsei University, Professor (E-mail: applymkk@yonsei.ac.kr)

The manuscript for this paper was submitted for review on August 21, 2002.

fundamental solution and a FE-BE coupling method, they developed an analytical approach which can be used to perform seismic response analysis of a soil with a horizontal layered structure. Although the methods of one-dimensional ground response analysis are useful for level or gently sloping sites with parallel material boundaries, such conditions are not commonly met. Therefore, multi-dimensional seismic response analysis techniques are required for characterizing the basin effects which are multi-dimensional by nature.

An analytical method for characterizing the basin effect in two-dimensional layered soil systems is presented in this study. This method is based on a FE-BE coupling technique following Kim *et al*. (2000). The near field is modeled by finite elements whereas the far field is modeled by the boundary element formulation using the multi-layer dynamic fundamental solution that satisfies the radiation condition of waves. For verification of the proposed method, a one-dimensional problem is modeled and the results are compared with those of the SHAKE program. Two dimensional seismic response analyses are then performed for various ground systems to study the basin effect, viz., the ground amplification. Effects of the ground geometry and material contrast on the seismic responses of ground systems are discussed in some detail.

2. Equations of Motion for Ground Response Analysis

Consider a soil-structure interaction system where a single structure is embedded in a half-plane soil subjected to an earthquake excitation as shown in Fig. 1. To derive the basic equation of motion, the structure is discretized schematically as shown. Subscripts are used to denote the nodes of discretized system. The nodes located on structure-soil interface are denoted by *b* and the remaining nodes of the structure by *s*. The substructure system is divided into the structural system and the excavated soil. To differentiate between the various subsystems, superscripts are used when necessary. The structure is indicated by the superscript *s* and the excavated far field soil by *g*. The soil without excavation, so-called free field, is denoted by *f* whereas *e* is used to designate the excavated near field soil. The equation of motion can be formulated in the frequency domain as follows (Wolf, 1985):

$$\begin{bmatrix} [S_{ss}\ (\omega)] & [S_{sb}\{\omega\}] \\ [S_{bs}\ (\omega)] & [S^s_{bb}\{\omega\}] \end{bmatrix} \begin{Bmatrix} \{u^t_s(\omega)\} \\ \{u^t_b(\omega)\} \end{Bmatrix} = \begin{Bmatrix} \{P_s(\omega)\} \\ -\{P_b(\omega)\} \end{Bmatrix} \quad (1)$$

where $\{u^t_s(\omega)\}$ and $\{u^t_b(\omega)\}$ are the amplitudes of the total displacements of the structure and the structure-soil

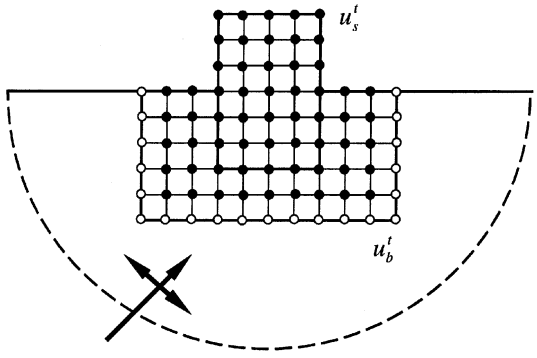

Fig. 1 Soil-Structure Interaction System

interface. The dynamic-stiffness matrix $[S(\omega)]$ of the structure can be decomposed into the submatrices $[S_{ss}(\omega)]$, $[S_{sb}(\omega)]$ and $S_{ss}(\omega)$. Also, $\{P_s(\omega)\}$ and $\{P_b(\omega)\}$ denote respectively the amplitude of load and interaction force applied to the ground. It is not easy to determine the impedance (dynamic-stiffness) matrix of the excavated far field soil $[S^g_{bb}(\omega)]$ since the domain of soil is unbounded. For earthquake excitation, the nodes not in contact with soil are not loaded, so the top half of Eq. (1) can be written by setting $\{P_s\} = \{0\}$ as follows:

$$[[S_{ss}(\omega)][S_{sb}(\omega)]] \begin{Bmatrix} \{u^t_s(\omega)\} \\ \{u^t_b(\omega)\} \end{Bmatrix} = \{0\} \quad (2)$$

Both substructures contribute to the dynamic equilibrium equations of the nodes *b* lying on the structure-soil interface. The contribution of the soil is discussed first. For the displacement $\{u^g_b(\omega)\}$, the interaction forces acting in the nodes *b* arising from the excavated soil vanish as, for this loading state, the line that is to subsequently form the structure-soil interface is a free surface. The interaction forces of the soil will thus depend on the motion relative to $\{u^g_b(\omega)\}$ such that

$$\{P_b(\omega)\} = [S^g_{bb}(\omega)](\{u^t_b(\omega)\} - \{u^g_b(\omega)\}) \quad (3)$$

Upon substitution of Eq. (3) into Eq. (1), the equations of motion for the nodes in contact with the soil become

$$[S_{bs}(\omega)]\{u^t_b(\omega)\} + [S^s_{bb}(\omega)]\{u^t_b(\omega)\} + [S^g_{bb}(\omega)](\{u^t_b(\omega)\} - \{u^g_b(\omega)\}) = \{0\} \quad (4)$$

By combining Eqs. (4) and (1), the equation of motions of the total structure-soil system can be written as

$$\begin{bmatrix} [S_{ss}(\omega)] & [S_{sb}(\omega)] \\ [S_{bs}(\omega)] & [S^s_{bb}(\omega)] + [S^g_{bb}(\omega)] \end{bmatrix} \begin{Bmatrix} \{u^t_s(\omega)\} \\ \{u^t_b(\omega)\} \end{Bmatrix}$$

$$= \begin{Bmatrix} \{0\} \\ [S^g_{bb}(\omega)]\{u^g_b(\omega)\} \end{Bmatrix} \quad (5)$$

In this formulation, the earthquake excitation is characterized by $\{u^g_b(\omega)\}$ which represents the motion of the nodes of excavated ground. In the behavior, so-called "scattered" motion, it is difficult to determine the value of $\{u^g_b(\omega)\}$. However, $\{u^g_b(\omega)\}$ may be replaced with $\{u^f_b(\omega)\}$ which is the displacement in free field motion and does not depend on excavation.

The impedance matrix and displacement vector in free field can be denoted by $[S^f_{bb}(\omega)]$ and $\{u^f_b(\omega)\}$, respectively. The dynamic stiffness matrix of the excavated near field part is written as $[S^e_{bb}(\omega)]$. Accordingly, the impedance matrix of the free-field can be written as follows:

$$[S^f_{bb}(\omega)] = [S^e_{bb}(\omega)] + [S^g_{bb}(\omega)] \quad (6)$$

As the excavated soil is regarded as one structure, the following relations hold.

$$[S_{bs}(\omega)] = [0] \quad (7)$$

$$[S^s_{bb}(\omega)] = [S^e_{bb}(\omega)] \quad (8)$$

$$\{u^t_b(\omega)\} = \{u^f_b(\omega)\} \quad (9)$$

Therefore, Equation (5) can be written as follows:

$$([S^e_{bb}(\omega)] + [S^g_{bb}(\omega)])\{u^f_b(\omega)\} = [S^g_{bb}(\omega)]\{u^g_b(\omega)\} \quad (10)$$

Introducing Eq. (6) into Eq. (10) leads to

$$[S^f_{bb}(\omega)]\{u^f_b(\omega)\} = [S^g_{bb}(\omega)]\{u^g_b(\omega)\} \quad (11)$$

Substitution of Eq. (11) in Eq. (5) results in the following discretized equations of motion.

$$\begin{bmatrix} [S_{ss}(\omega)] & [S_{sb}(\omega)] \\ [S_{bs}(\omega)] & [S^s_{bb}(\omega)] + [S^g_{bb}(\omega)] \end{bmatrix} \begin{Bmatrix} \{u^t_s(\omega)\} \\ \{u^t_b(\omega)\} \end{Bmatrix} = \begin{Bmatrix} \{0\} \\ [S^f_{bb}(\omega)]\{u^f_b(\omega)\} \end{Bmatrix} \quad (12)$$

The amount of interaction of the embedded part described by the l.h.s. of Eq. (12) depends on $[S^s_{bb}(\omega)] + [S^g_{bb}(\omega)]$, which, after making use of Eq. (6), is equal to

$$[S^s_{bb}(\omega)] + [S^g_{bb}(\omega)] = [S^s_{bb}(\omega)] - [S^e_{bb}(\omega)] + [S^f_{bb}(\omega)] \quad (13)$$

The difference of the property matrix of the structure and of the soil in the embedded region $[S^s_{bb}(\omega)] - [S^e_{bb}(\omega)]$ is thus of importance. Using Equation (13), Equation (12) can be reformulated as follows:

$$\begin{bmatrix} [S_{ss}(\omega)] & [S_{sb}(\omega)] \\ [S_{bs}(\omega)] & [S^s_{bb}(\omega)] - [S^e_{bb}(\omega)] + [S^f_{bb}(\omega)] \end{bmatrix} \begin{Bmatrix} \{u^t_s(\omega)\} \\ \{u^t_b(\omega)\} \end{Bmatrix} = \begin{Bmatrix} \{0\} \\ [S^f_{bb}(\omega)]\{u^f_b(\omega)\} \end{Bmatrix} \quad (14)$$

From the relationship of the excavated soil and the free field, the scattered earthquake excitation $\{u^g_s(\omega)\}$ can be presented as follows:

$$\{u^g_s(\omega)\} = [S^g_{bb}(\omega)]^{-1}[S^f_{bb}(\omega)]\{u^f_b(\omega)\} \quad (15)$$

However, it is unnecessary to determine this motion of the soil modified by the excavation since $\{u^g_s(\omega)\}$ and $\{u^g_b(\omega)\}$ do not exist in a real soil-structure interaction system.

3. Numerical Formulation

3.1 Finite Element Formulation for Near Field

The governig equations of motion of the near field in frequency domain can be written as the following:

$$[S^{FE}(\omega)]\{u^{FE}(\omega)\} = \{F^{FE}(\omega)\} \quad (16)$$

where $[S(\omega)]\{u(\omega)\}$ and $\{F(\omega)\}$ is the impedence matrix, displacement vector and force vector, respectively. Superscript *FE* denotes the finite-element formulation. The impedence matrix is given by the following equation:

$$[S^{FE}(\omega)] = [K^*] + i\omega[C] - \omega^2[M] \quad (17)$$

where $[K^*], [C]$ and $[M]$ are the static stiffness matrix, damping matrix and mass matrix, respectively.

3.2 Boundary Element Formulation for Far Field

The far field is modeled by the boundary element formulation based on the dynamic fundamental solution in the frequency domain. The fundamental solution satisfies the radiation condition in multi-layered half-plane. The displacement of the dynamic fundamental solution of multi-layered half-plane is given as follows (Rhee, 1998, Kim *et al*., 2000):

$$u^l_{pq}(\omega, x, z, z_s) = \frac{1}{2\pi}\left[\int_{-a}^{+a}\{(\boldsymbol{D}^j_{nq})e^{-ikx^*}\}dx + \int_{-\infty}^{-a}\{(\tilde{\boldsymbol{D}}^j_{nq})e^{-ikx^*}\}dx + \int_{+a}^{+\infty}\{(\tilde{\boldsymbol{D}}^j_{nq})e^{-ikx^*}\}dx \right. \quad (18)$$

where $\boldsymbol{D}^j_{nq}$ is the displacement vector and stress vector of

the *j*-th layer, subscript n is the direction of the displacement, *q* is the direction of the applied force, *k* is the wave number and x^* is horizontal distance between the source and receiver, respectively. In Equation (18), $\tilde{\boldsymbol{D}}^j_{nq}$ is the asymptotic solution of $\boldsymbol{D}^j_{nq}$. The integrand term in the above equation is the function of depth *z* including $e^{-k(z-ix)}$. In Equation (18), the analytical integrations of asymptotic solutions are performed within the range $(-\infty, -a)$ and $(+a, +\infty)$, and the numerical integrations within the range $(-a, +a)$. The value *a* indicates the wavenumber at which the numerical solutions converge sufficiently to the asymptotic solutions. The value *a* is generally taken as 1.5~2.0 times of Rayleigh wavenumber as suggested by the parametric studies (Rhee, 1999).

Numerical fundamental solutions of multi-layered half-planes are applied to the boundary integral equations (Brebbia *et al*., 1985) as follows:

$$c_{ij}u_j(\omega,x,y) + \int_\Gamma p^*_{ij}(\omega,x,y)u_j(\omega,x,y)d\Gamma = \int_\Gamma u^*_{ij}(\omega,x,y)p_j(\omega,x,y)d\Gamma,\ \ i,\ j = x,\ y \tag{19}$$

where superscript * represents the form of fundamental solutions directly applicable to the boundary integral equations, *i* is the direction of a unit load, *j* is the direction of the displacement and traction on the integral path Γ, and c_{ij} is a constant determined from the geometry of the boundary. The displacement $u^*_{ij}(\omega,x,y)$ and the traction $p^*_{ij}(\omega,x,y)$ are obtained numerically. The displacements and stresses at each node are calculated by discretizing the boundary using Eq. (19).

In the boundary element region, the system equation has the following relation:

$$[H^{BE}(\omega)]\{u^{BE}(\omega)\} = [G^{BE}(\omega)]\{p^{BE}(\omega)\} \tag{20}$$

where $\{u^{BE}(\omega)\}$ and $\{p^{BE}(\omega)\}$ are the nodal displacement and surface force vector, respectively, and the superscript *BE* represents the region discretized by the boundary element. Eq. (20) can be recast as the following equation:

$$[S^{BE}(\omega)]\{u^{BE}(\omega)\} = \{F^{BE}(\omega)\} \tag{21}$$

where $[S^{BE}(\omega)]$ is the impedance matrix composed of $[H^{BE}(\omega)]$ and $[G^{BE}(\omega)]$, $\{u^{BE}(\omega)\}$ is the vector of unknown displacement, and $\{F^{BE}(\omega)\}$ is the load vector.

3.3 FE-BE Coupling

The impedance matrices $[S^{FE}(\omega)]$ and $[S^{BE}(\omega)]$ are of the same form so that FEM and BEM can be coupled as follows:

$$[[S^{FE}(\omega)]+[S^{BE}(\omega)]]+\{\{u^{FE}(\omega)\}+\{u^{BE}(\omega)\}\} = \{\{F^{FE}(\omega)\}+\{F^{BE}(\omega)\}\} \tag{22}$$

or

$$[S^G(\omega)]\{u^G(\omega)\} = \{F^G(\omega)\} \tag{23}$$

where $[S^G(\omega)]$ is the coupled dynamic impedance matrix, $\{u^G(\omega)\}$ is the coupled displacement vector and $\{F^G(\omega)\}$ is the coupled external load vector. The numerical analysis may then be performed for each frequency and time domain responses can be obtained by using the inverse FFT technique.

4. Validation of Method

The most commonly used ground response analysis technique is the one-dimensional method using the wave propagation theory. SHAKE (Schnabel, *et al*., 1972) is one of the well known computer programs for seismic response analysis using the one dimensional theory. In order to validate the approach proposed herein, the ground response analysis is performed and the results are compared with these of SHAKE. The structure of the soil system and the material properties are shown in Fig. 2 and Table 1, respectively. The time history of input motion used in the analysis is shown in Fig. 3.

The results of the linear analysis are shown in Fig. 4. Fig. 4(a) shows the results of SHAKE and Fig. 4(b) the results of this study. As seen in the Figures, the two results seem to agree fairly well. The maximum ground accelerations from SHAKE and this study are given by 0.177 g and 0.171 g, respectively, and the difference is about 4%. Fig. 5 shows the results in the frequency domain. Again, the frequency response of the present study is in good agreement with that of SHAKE.

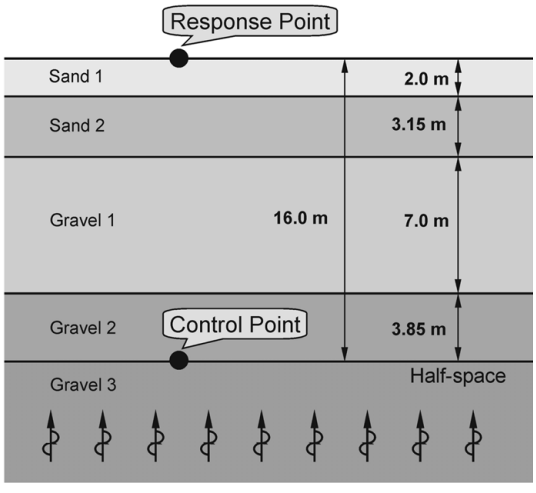

Fig. 2 Ground Shape for the Verification Analysis

Table 1. Soil Properties for the Verification of Ground Response Analysis

Soil Type	Depth (m)	Shear wave velocity (m/s)	Density (kg/m^3)	Young's Modulus (MPa)	Poisson's Ratio	Damping Ratio
Sand 1	0-2	133	1.69×10^3	82	0.3	0.02
Sand 2	2-5.15	231	1.93×10^3	304	0.3	0.02
Gravel 1	5.15-12.15	317	2.42×10^3	714	0.3	0.02
Gravel 2	12.15-16	476	2.42×10^3	1,612	0.3	0.02
Gravel 3	16- ∞	476	2.42×10^3	1,612	0.3	0.02

5. Ground Response Analysis For Alluvial Basins

5.1 Effect of the Ground Geometry

In order to study the site effect, a two-dimensional ground response analysis is performed for a fictitious basin type alluvium which is shown in Fig. 6(a). As shown in the figure, the ground is a 30 m wide and 10 m deep semicircular alluvial soil deposit in a soft rock layer. Ground response analysis is also performed for a similar but horizontally layered soil system as shown in Fig. 6(b) for comparison. The soil properties are tabulated in Table 2. The seismic input motion as given in Fig. 3 is applied at 30 m deep from the surface of the base rock. The time history of the ground acceleration is shown in Fig. 7 whereas and the frequency response in Fig. 8. The maximum ground acceleration re−sponses for the two cases are shown in Fig. 9. As shown in the Figures, the responses of the alluvial soil are increased or "amplified" over that of the layered soil: by some 49%. This suggests that the ground response analysis based on localized ground inspection data can lead to inaccurate results.

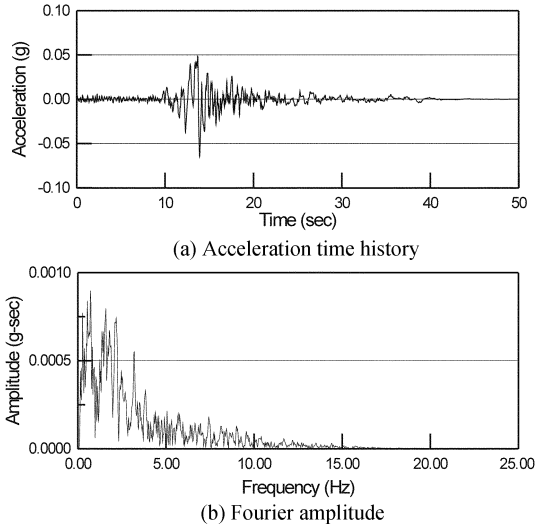

(a) Acceleration time history

(b) Fourier amplitude

Fig. 3 Ground Surface Motion at Yerba Buena Island in the 1989 Loma Prieta Earthquake

5.2 Effects of the Basin Material

To compare the basin effect due to the changes of material properties, the ground response analysis is performed for the ground model shown in Fig. 6(a) for three different

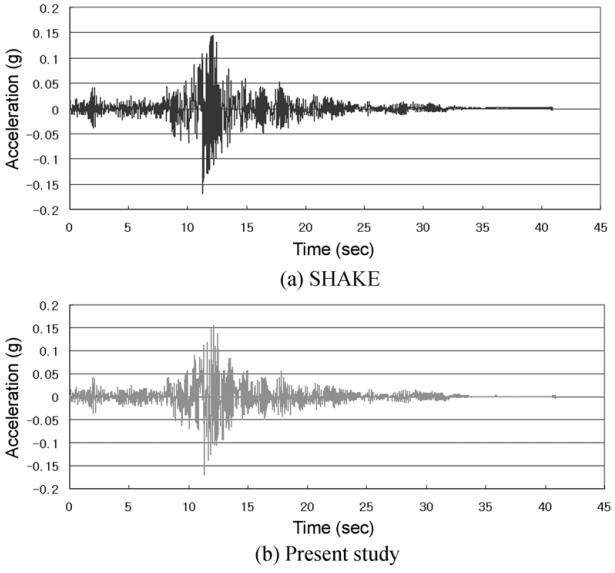

(a) SHAKE

(b) Present study

Fig. 4 Ground Responses in Linear Case (Time Domain)

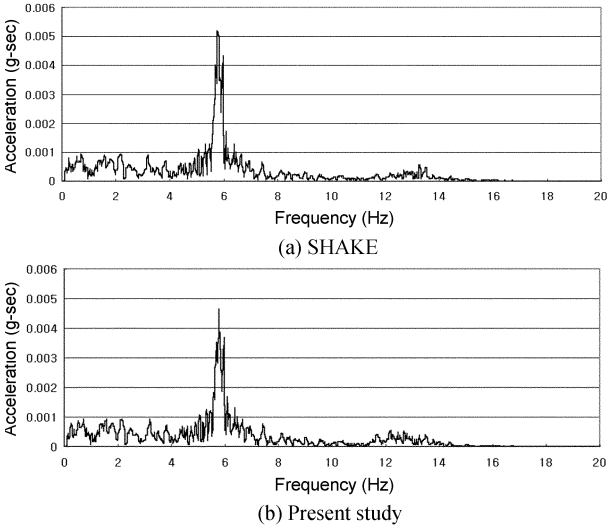

(a) SHAKE

(b) Present study

Fig. 5. Ground Responses in Linear Case (Frequency Domain)

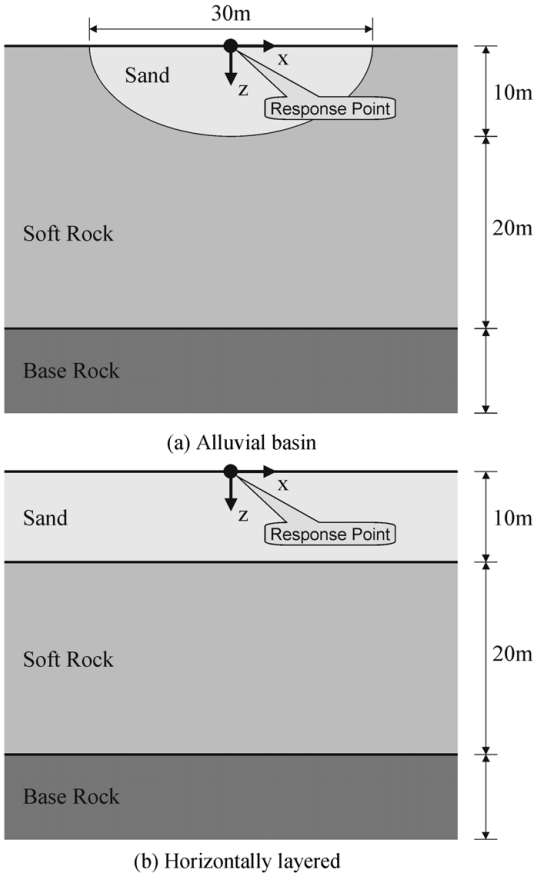

Fig. 6 Geometry of the Soil

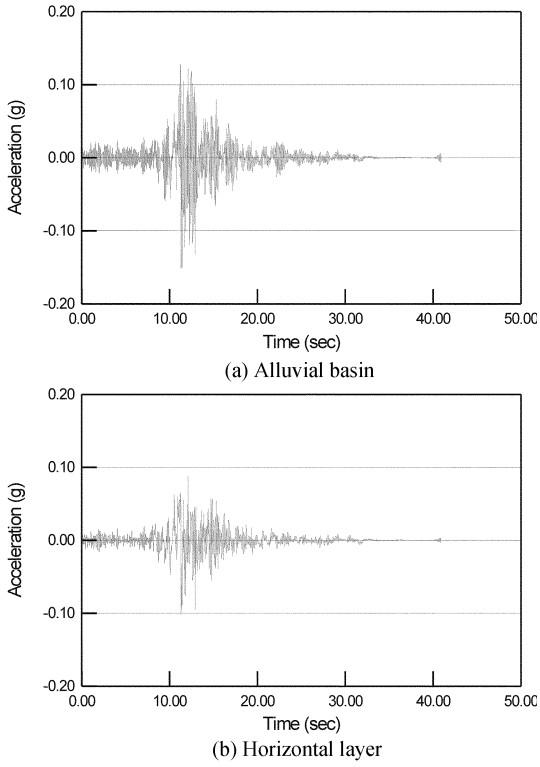

Fig. 7. Calculated Acceleration Time Histories

shear wave velocities of the basin. Soil properties used in the calculation are tabulated in Table 3. The seismic input motion is the same as before. The maximum acceleration responses on the surface are plotted as a function of the distance from the origin for the three cases in Fig. 10. As shown in the figures, the maximum responses are increased as the shear wave velocities are decreased. This suggests that, when the basin is filled with soft soil, the ground amplification can be quite significant.

6. Conclusions

A numerical method for seismic ground response analysis in multi-layered semi-infinite media is developed. The

Table 2. Soil Properties of the Ground Response Analysis

Soil Type	Depth (m)	Shear wave velocity (m/s)	Density (kg/m^3)	Young's Modulus (MPa)	Poisson's Ratio	Damping Ratio
Sand	0-10	150	1.8×10^3	109	0.35	0.02
Weathered Rock	10-30	300	2.0×10^3	468	0.30	0.02
Base Rock	30- ∞	1000	2.75×10^3	6,875	0.25	0.02

Table 3. Soil Properties of the Ground Response Analysis due to the Soil Property

Soil Type	Depth (m)	Shear wave velocity (m/s)	Density (kg/m^3)	Young's Modulus (MPa)	Poisson's Ratio	Damping Ratio
Sand	0-10	200	1.8×10^3	187	0.3	0.02
		300		421		
		400		748		
Weathered Rock	10-30	500	2.0×10^3	1,300	0.3	0.02
Base Rock	30- ∞	1000	2.7×10^3	7,020	0.3	0.02

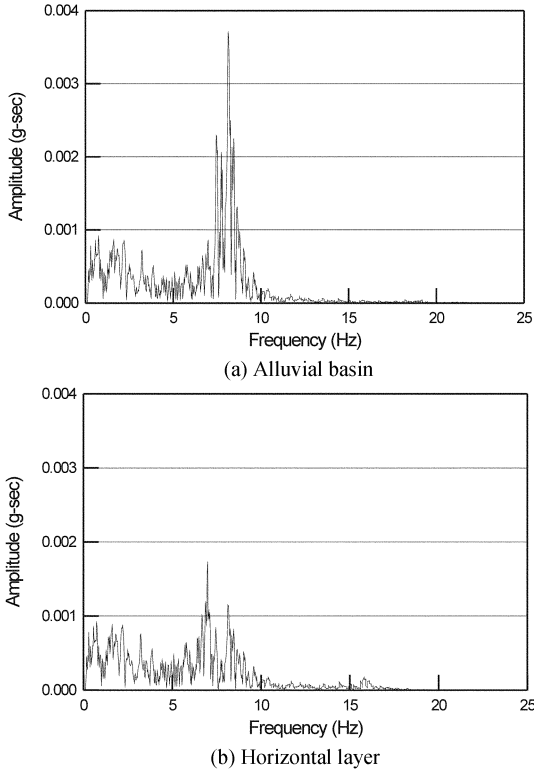

Fig. 8 Calculated Frequency Domain Responses

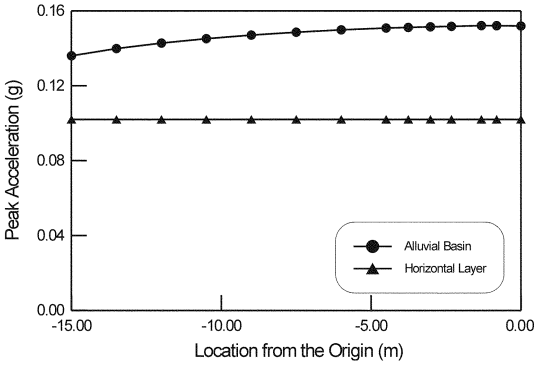

Fig. 9. Peak Ground Acceleration Responses

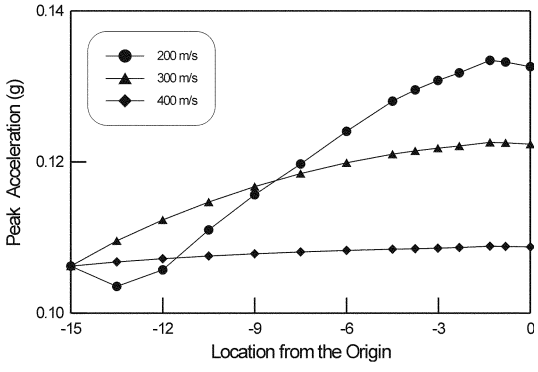

Fig. 10. Peak Acceleration Responses for Three Types of Alluvial Soil

near field is modeled by the finite element method and the far field is modeled by a boundary element formulation based on a newly developed dynamic fundamental solution. In order to validate the analytical approach, one dimensional free field response analysis is performed and results are compared with these of a well known code. Two dimensional seismic response analyses are then performed for various ground systems to study the basin effect. Effects of the basin geometry and the material contrasts on the seismic responses are discussed through numerical examples. It is shown that the 2D nature of the basin effect can not be captured with the traditional 1D analysis. The results also suggest that the ground amplification can be significant especially when the basin is filled with a soft soil.

References

Bielak, J., Hisada, Y., Bao, H., Xu, J., and Ghattas, O. (2000). "One- vs. two- or three-dimensional effects in sedimentary valleys." *12th World Conference on Earthquake Engineering*, Paper No. 2689, Auckland, Australia.

Bielak, J., Xu, J., and Ghattas, O. (1999). "Earthquake ground motion and structural response in alluvial valleys." *Journal of Geotechnical and Geoenvironmental Engineering*, Vol. 125, No. 5, May, pp. 413-425.

Brebbia, C.A., Telles, J.C.F., and Wrobel, L.C. (1983). *Boundary Element Techniques*, Springer-Verlag, NY.

Gazetas, G. (1987). "Seismic response of earth dam; some recent developments." *Soil Dynamics and Earthquake Engineering*, Vol. 6, No. 1, pp. 3-47.

Kim, M.K., Lim, Y.M., Kim, M.K., and Rhee, J.W. (2001). "Free field response analysis using dynamic fundamental solution." *Journal of the Earthquake Engineering Society of Korea*, Vol. 5, No. 2, pp. 83-91. (in Korean)

Kim, M.K., Lim, Y.M., and Rhee, J.W. (2000). "Dynamic analysis of layered half planes by coupled finite and boundary elements." *Engineering Structures*, Vol. 22, pp. 670-680.

Reinoso, E., Wrobel, L.C., and Powel, H. (1997). "Two-dimensional scattering of P, SV and rayleigh waves: preliminary results for the valley of mexico." *Earthquake Engineering and Structural Dynamics*, Vol. 26, pp. 595-616.

Rhee, J.W. (1998). *Boundary element analysis of soil-structure interaction using dynamic fundamental solutions on multi-layered half-planes,* Ph.D. dissertation, Yonsei University, Seoul, Korea. (in Korean)

Rhee, J.W., Kim, M.K., Park, S.W., and Kim, M.K. (1999). "Effects of the dynamic cross-interaction in layered half-planes by FE-BE coupling." *First International Conference on Advances in Structural Engineering and Mechanics*, Seoul, Korea.

Schnabel, P.B., Lysmer, J., and Seed, H.B. (1972)., "SHAKE: A computer program for earthquake response of horizontally layered sites." *Report No. EERC/72-12*, Earthquake Engineering Research Center, Univ. of California, Berkeley.

Wolf, J.P. (1985). *Dynamic Soil-Structure Interaction*, Prentice-Hall, NJ